

## Nanotechnology

## "Click" Chemistry Mildly Stabilizes Bifunctional Gold Nanoparticles for Sensing and Catalysis

Na Li,<sup>[a]</sup> Pengxiang Zhao,<sup>[b]</sup> Na Liu,<sup>[c]</sup> María Echeverría,<sup>[d]</sup> Sergio Moya,<sup>[d]</sup> Lionel Salmon,<sup>[e]</sup> Jaime Ruiz,<sup>[a]</sup> and Didier Astruc<sup>\*[a]</sup>

**Abstract:** A large family of bifunctional 1,2,3-triazole derivatives that contain both a polyethylene glycol (PEG) chain and another functional fragment (e.g., a polymer, dendron, alcohol, carboxylic acid, allyl, fluorescence dye, redox-robust metal complex, or a  $\beta$ -cyclodextrin unit) has been synthesized by facile "click" chemistry and mildly coordinated to nanogold particles, thus providing stable water-soluble gold

nanoparticles (AuNPs) in the size range 3.0–11.2 nm with various properties and applications. In particular, the sensing properties of these AuNPs are illustrated through the detection of an analogue of a warfare agent (i.e., sulfur mustard) by means of a fluorescence "turn-on" assay, and the catalytic activity of the smallest triazole–AuNPs (core of 3.0 nm) is excellent for the reduction of 4-nitrophenol in water.

## Introduction

Gold nanoparticles (AuNPs) have emerged as a key field of nanoscience due to their quantum-related and supramolecular properties,<sup>[1]</sup> with promising applications in catalysis,<sup>[2]</sup> sensing,<sup>[3]</sup> and nanomedicine, in particular.<sup>[4]</sup> A variety of ligands have been shown to stabilize AuNPs since the citrate method of synthesis reported in 1952 by Turkevich et al. that allowed the formation of water-soluble AuNPs in the range 15–50 nm, which are still currently used in biomedical applications.<sup>[5]</sup> Sulfur ligands are popular stabilizers, in particular thiolate ligands in the Brust–Schiffrin method, which provide small monodisperse AuNPs (2–6 nm).<sup>[6]</sup> Cetyltrimethylammonium bromide (CTAB),<sup>[7]</sup> a remarkable Au-nanorod stabilizer, has restrictions in biological applications due to the biotoxicity of this free surfactant.<sup>[8]</sup> Besides, many other nitrogen donors, such as imidazoles,<sup>[9]</sup> pyridines,<sup>[10]</sup> and others, have also been introduced for the stabilization of AuNPs, with the advantage of

a modest AuNP–ligand bond strength that allows the AuNP surface to be reached by ready ligand displacement. Such an introduction of substrates onto the AuNP surface upon weak ligand displacement leads to possibilities in optical, sensing, and catalytic applications.<sup>[11]</sup> For AuNP stabilizers, the use of a large class of biocompatible neutral and water-solubilizing ligands that are heterobifunctional is now considered to be a new, general, and environmentally friendly strategy that can produce a variety of side products and overcome the limitations indicated above.

The Cu<sup>I</sup>-catalyzed azide–alkyne cycloaddition (CuAAC) reaction ("click" reaction) is one of the most well-known methods of linking functionalities,<sup>[12]</sup> and this reaction forms 1,4-heterobifunctional 1,2,3-triazoles, which are very useful ligands. The 1,2,3-triazole ring is an amphoteric  $\pi$ -electron-rich aromatic, which is completely biocompatible and stable toward both oxidizing and reducing agents. So far, click chemistry has been one of the numerous methods to functionalize thiolate ligands of nanoparticles.<sup>[13]</sup> Herein, we show that the clicked 1,2,3-triazoles can be used as excellent neutral ligands to stabilize AuNPs with the following great advantages: 1) these ligands are neutral and mild and involve a weaker bond with the AuNP cores than the thiolate ligands, a property that will be shown to be crucial in sensing and catalysis; 2) the great potential of click synthesis allows the introduction of a large variety of functional groups; 3) the heterobifunctionality of the 1,2,3-triazole ligands synthesized by click reactions allows the introduction of two functional groups at a time, which makes them superior to, for instance, thiolate and amine ligands; 4) water-soluble AuNPs can be synthesized in this way by choosing the biocompatible polyethylene glycol (PEG) group as one of the triazole substituents, whereas the other substituent will lead to a specific property, function, and application in water. The 1,2,3-triazole ring can associate with AuNP surfaces through the lone pair of electrons on the sp<sup>2</sup>-hybridized nitro-

[a] N. Li, Dr. J. Ruiz, Prof. Dr. D. Astruc  
ISM, UMR CNRS 5255  
Université Bordeaux, 351 Cours de la Libération  
33405 Talence Cedex, (France)  
E-mail: d.astruc@ism.u-bordeaux1.fr

[b] Dr. P. Zhao  
Science and Technology on Surface Physics and Chemistry Laboratory  
PO Box 718-35, Mianyang 621907, Sichuan (China)

[c] Dr. N. Liu  
ICMCB, UPR CNRS 9048, Université Bordeaux, 87 Avenue  
Pey-Berland, 33608 Pessac Cedex (France)

[d] M. Echeverría, Dr. S. Moya  
CIC biomaGUNE, Paseo Miramónn°182, Edif. "C"  
20009 Donostia-San Sebastián (Spain)

[e] Dr. L. Salmon  
LCC, UPR CNRS 8241, 205 Route de Narbonne  
31077 Toulouse Cedex (France)

Supporting information for this article is available on the WWW under <http://dx.doi.org/10.1002/chem.201402652>.

gen atoms.<sup>[14]</sup> In addition, dendrimers that incorporate triazole rings have been shown to have an excellent ability to encapsulate and stabilize noble-metal NPs.<sup>[15]</sup>

These new 1,2,3-triazole–AuNPs synthesized in this study with a biologically benign PEG chain ( $M_w=2000$ ) and various useful functional groups are anticipated to potentially undergo various applications based upon their electrochemical, optical, fluorescent, supramolecular, encapsulating, and catalytic properties. For the purpose of utilizing the properties of triazole–AuNPs, including the properties of the ligand and AuNP core, each compound contains two groups on each triazole unit, that is, a solubilizing PEG chain and a functional fragment.

## Results and Discussion

### Design of bifunctional triazole-stabilized AuNPs

The functional fragments of 1–5 include polymeric and dendronic groups with various functionalities (Figure 1). A coumarin fragment, which was expected to have excellent photoluminescence properties, was introduced in 6.

Redox-robust organometallic compounds that contain a ferrocenyl group, tris-ferrocenyl dendron, or the “electron-reservoir” complex  $[\text{CpFe}(\eta^6\text{-C}_6\text{Me}_6)][\text{PF}_6]$  (Cp = cyclopentadienyl) complex<sup>[16]</sup> were introduced to combine electrochemical and

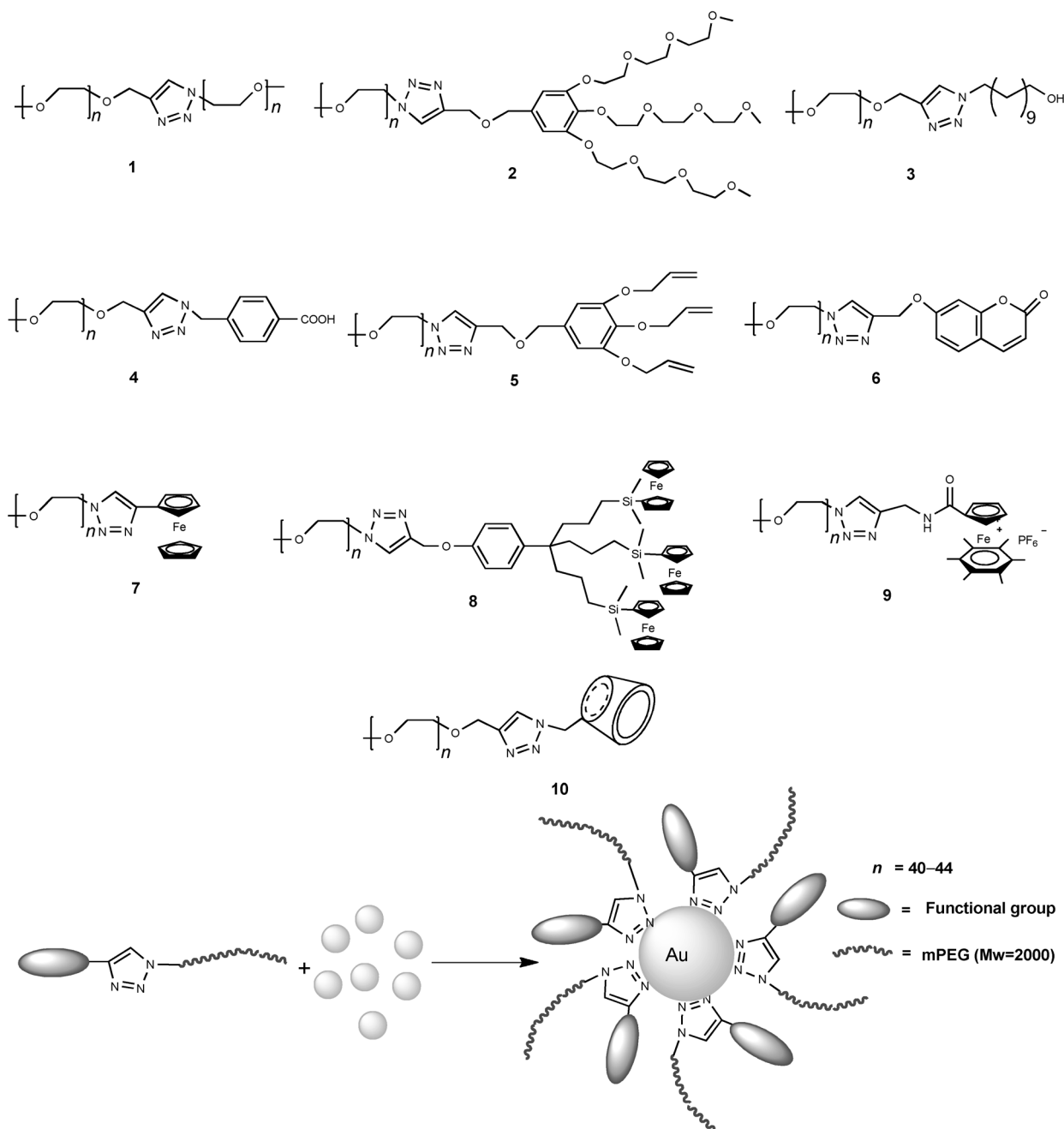


**Figure 1.** Structures of the disubstituted 1,2,3-triazoles 1–10, and the stabilization of AuNPs with these disubstituted 1,2,3-triazole molecules. mPEG = methoxy-polyethylene glycol.

optical properties in triazole–AuNPs in **7–9**, respectively (Figure 1). These iron sandwich complexes are redox catalysts that have been used as glucose biosensors in the case of ferrocene<sup>[16b,c]</sup> and as redox catalysts for the reduction of nitrate and nitrite moieties in water in the case of the mixed sandwich complex. The presence of a large number of these species in water-soluble NPs should further facilitate their use as redox catalysts and redox sensors. In addition, **10** has been assembled with a  $\beta$ -cyclodextrin ( $\beta$ -CD) unit, that is, a rigid cylindrical amphiphilic molecule, and has been extensively used to include hydrophobic molecules, such as anticancer drugs, to increase their solubility in water. Hence, **AuNP-10** is a promising candidate for drug-delivery vehicles. The synthesis of the disubstituted triazole-stabilized AuNPs was conducted by using tetrachloroauric acid and a 1,2,3-triazole dissolved in deionized water in a standard molar ratio 1:2 of Au<sup>III</sup>/triazole (**AuNP-6** = 1:0.5, **AuNP-2** = 1:5) and followed by the addition of sodium borohydride as the reductant.

### Characterization of the AuNPs

The triazole–AuNPs were characterized by using UV/Vis spectroscopy, TEM, and dynamic light scattering (DLS). Particular properties of **AuNP-5**, **-6**, **-7**, and **-10** with special functional groups were displayed separately from the corresponding measurements. The TEM images depict the core size of the AuNPs to be in the range 3.0–11.2 nm.

Variations in the core size relies on the ratio between the Au<sup>III</sup> center and the triazole in the preparation, and secondary determinants of this variation are the rate of reduction, which result from the addition of the reductant, and the slight influence of the distinctive functional fragments in each triazole compound. For instance, **AuNP-6** ( $d = 11.2$  nm) is much larger than other AuNPs because it was prepared with a ratio of Au<sup>III</sup>/triazole ligand of 1:0.5, thus leading to an assembly of the Au atoms that proceeds much faster than the AuNP stabilization by the triazole ligands until a certain point. In addition, a trace of anisotropic nanocrystals was produced during this synthesis (Figure 2). With a diameter over 10 nm, **AuNPs-6** should show prominent efficiency in fluorescence quenching assays. In contrast, **AuNPs-2** was prepared with a low Au<sup>III</sup>/triazole ratio (i.e., 1:5) to obtain smaller AuNPs that could reveal excellent catalytic properties. The AuNPs that were prepared with the ratio of Au<sup>III</sup>/triazole of 1:2 displayed similar diameters (**AuNPs-1** = 6.1, **AuNPs-4** = 6.0, **AuNPs-5** = 5.9, **AuNPs-8** = 5.2, **AuNPs-9** = 5.7, **AuNPs-10** = 5.2 nm), except for **AuNPs-3** and **AuNPs-7** (4.0 and 3.8 nm, respectively). The location of the surface plasmon band (SPB) in the UV/Vis spectra (see the Supporting Information for details) of various AuNPs corresponds well to the core-size distribution of these AuNPs.

The behavior of **AuNP-1–AuNP-10** in water were revealed through DLS analysis. The diameter obtained for each AuNP is subjected to deviations according to the nature of the functional groups (see the Supporting Information). **AuNP-1** agglomerates in a large cluster, which includes many individual AuNPs due to extensive aggregating supramolecular interactions among the PEG tails of both triazole substituents ( $d =$

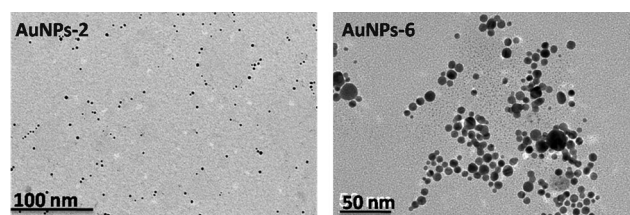


Figure 2. TEM images of **AuNP-2** and **AuNP-6** (core diameter = 3.0 and 11.2 nm, respectively).

396 nm) in aqueous solution. The PEG chains dominate the behavior of the AuNPs in solution because of their long flexible chain and interweave with one another among several adjacent AuNPs. On the other hand, **AuNP-2–AuNP-6** that contain organic fragments on one triazole substituent only give mobility diameters in the range 140–250 nm because intermolecular PEG-chain interweaving proceeds only on one triazole side. Finally, **AuNP-7–AuNP-9** that bear a ferrocenyl unit and related groups are well dispersed in water and show a mobility diameter of lower than 30 nm (see Figures S48, S50, and S51 in the Supporting Information). Consequently, it is concluded that the ferrocenyl group and its derivatives inhibit the gathering of individual AuNPs.

The electrochemical properties of **AuNP-7** were recognized upon recording cyclic voltammograms (see Figure S50 in the Supporting Information). Both the electrochemical and optical properties of **AuNP-7** have proven to be valuable for the design of sensory devices that are devoted to the selective recognition of extensively studied oxo anions (especially  $\text{HSO}_4^-$ ,  $\text{H}_2\text{PO}_4^-$ , and  $\text{ATP}^{2-}$  ions).<sup>[17]</sup>

The surface-enhanced Raman scattering (SERS) effect of triazole–AuNPs was investigated by comparison between the Raman spectra of **5** and **AuNP-5** (Figure 3). This comparison shows a distinct enhancement at  $\lambda = 539$  (N–N wagging) and  $1100\text{ cm}^{-1}$  (C–N, C=C, and N=N stretching), both of these signals correspond to the triazole ring.<sup>[14b,c]</sup> In the Raman spectrum of **AuNP-5**, these two signals of the triazole ring were so

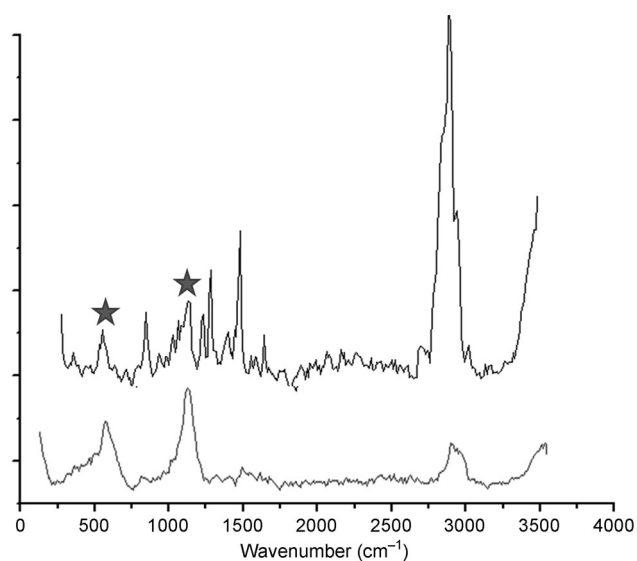


Figure 3. Raman spectra of **5** (upper curve) and **AuNP-5** (lower curve).

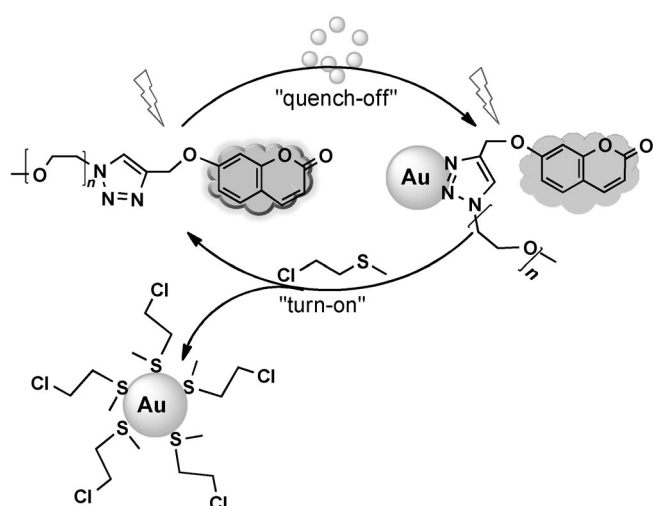
drastically amplified that one cannot clearly distinguish the other signals relative to the same position in the spectrum of **5**.

This phenomenon shows that the triazole C–N and N=N bonds are much closer to the AuNPs surface than any other part of the triazole group. Therefore, this finding indicates that the triazole neutral ligands stabilize the AuNPs by coordination of their nitrogen atoms to the AuNP surface.

These AuNPs are thermally stable at 100 °C in aqueous solution, which is indicated by the absence of plasmon-band variation after several hours at 100 °C (see Figure S46 in the Supporting Information), but these AuNPs agglomerate in the condensed phase, which inhibits thermogravimetric studies. Their stability to variations in pH values in aqueous solution was further studied by using UV/Vis spectroscopic analysis to record the SPB band of **AuNP-5** at 25 °C (see Figure S46 in the Supporting Information), whereby various pH values were adjusted by the addition of NaOH or HCl solution. As a result, no obvious plasmon-band shift was observed in the range pH 4–9, that is, the range of physiological pH values in the cellular environment, thus indicating that the triazole–AuNPs are stable in a physiological pH environment.

### Fluorescence sensing of 2-CEMS

Triazole–AuNPs were also used as excellent fluorescence quenchers for fluorescence-based assays because of their extraordinary high molar extinction coefficients and broad energy bandwidth. The fluorescent dye coumarin-containing triazole **6** exhibits fluorescence under UV light (Scheme 1). After combination with AuNPs, the fluorescence of the donor ligand is decreased or even totally quenched (see Figure S47 in the Supporting Information, which shows the photographs of the fluorescent **6** and **AuNP-6** under illuminance of UV light at  $\lambda = 365$  nm). Compound **6** displays an intense band with a wavelength of maximum emission  $\lambda_{\text{max}} = 472$  nm, in the



**Scheme 1.** A sketch that illustrates the fluorescence quenching of **6** by conjugation with AuNPs and the fluorescence “turn-on” detection of the sulfur-mustard analogue 2-CEMS through ligand displacement from the AuNP surface.

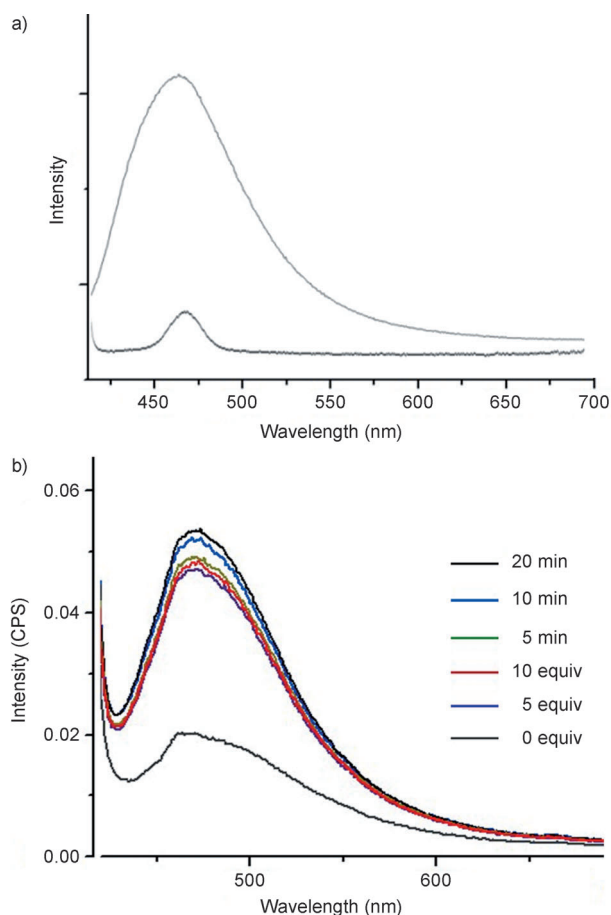


**Figure 4.** a) Emission spectra of **6** (0.4 mM, upper curve) and **AuNP-6** (0.4 mM, lower curve) in aqueous solution. b) Emission spectra of **AuNP-6** without titration of 2-CEMS, with 5 equivalents of 2-CEMS, with 10 equivalents of 2-CEMS, and 5, 10, and 15 min after the addition of 10 equivalents of 2-CEMS, respectively ( $\lambda_{\text{ex}} = 405$  nm).

emission spectrum with excitation at  $\lambda_{\text{ex}} = 405$  nm (Figure 4a). After stabilization of the AuNPs with **6** (see the preparation details in the Experimental Section), the fluorescent emission is dramatically quenched. The fluorescence quenching phenomenon is due to the short distance between the coumarin unit and the AuNPs surface, thus indicating that **AuNP-6** has potential applications in biosensing or metal-ion detection by using this fluorescence “turn-on” method upon the substitution of fluorescent ligands.

**AuNP-6** was employed in the fluorescent sensing of 2-chloroethyl methyl sulfide (2-CEMS), which is a widely employed analogue of bis(2-chloroethyl) sulfide (2-CEES), a mortiferous chemical weapon that is commonly known as “mustard gas” and was infamous in World War II. For security, the detection of 2-CEES has always been used instead of its less toxic analogues.<sup>[9b, 18]</sup> The sensing capability of **AuNP-6** was verified through a ligand-displacement process through progressive titration of a solution of 2-CEMS in methanol into a solution of **AuNPs-6** in water/methanol 7:3 in a standard quartz cuvette (path length: 1 cm), which were mixed by inversion for 10 seconds (see the Experimental Section). The obtained solution was recorded by means of fluorescence emission spectroscopy immediately or afterwards (Figure 4b). As expected, the fluo-

rescence band of **AuNP-6** raises with an increase of the 2-CEMS concentration. Indeed, a strong increase in band intensity was observed when 2-CEMS was added in a 10-fold concentration, and the ligand displacement reached equilibrium within 10 minutes of the titration.

As a comparison, the titration of 1-dodecanethiol was carried out by following the same procedure, and a similar performance was observed as monitored by emission spectroscopic analysis (see Figure S48 in the Supporting Information). Substitution of the triazole ligands by the sulfide or thiol analytes on the AuNP surface results in the release of fluorescence, which had been quenched by the AuNPs surface-energy-transfer effect. Facile bonding of the Au–triazole moiety to 2-CEMS means that the AuNPs can detect the chemical-warfare-agent sulfur mustard by using a fluorescence “turn-on” assay.

#### Catalytic performance of AuNPs-2 in the reduction of 4-nitrophenol

The reduction of 4-nitrophenol is widely used for the evaluation of the catalytic activity of various metal NPs owing to the high sensitivity of this reaction to the metal catalyst and the convenient determination of the reaction rate by UV/Vis spectroscopic analysis.<sup>[19]</sup> The triazole-stabilized **AuNP-2** with a core size of  $d=3.0$  nm (that is, smaller than other triazole–AuNPs) were probed as catalysts for the reduction of nitrophenol insofar as the AuNP surface was expected to be readily available for the activation of adsorbed substrates subsequent to the substitution of weakly coordinated triazole ligands by the substrates. Briefly, a solution of 4-nitrophenol (0.09  $\mu\text{mol}$ ) and sodium borohydride (7.5  $\mu\text{mol}$ ) in water was prepared in a standard quartz cuvette (3 mL). This solution immediately turned yellow and showed a strong absorption at  $\lambda=400$  nm in the UV/Vis spectrum. An aqueous solution of **AuNP-2** (0.5%) was injected into the quartz cuvette, and the reduction reaction was monitored by UV/Vis spectroscopic analysis (Figure 5).

The absorption of 4-nitrophenol at  $\lambda=400$  nm was shown to rapidly decrease with the reaction time (Figure 5a). The plot of the consumption rate of 4-nitrophenol  $-\ln(C/C_0)$  versus the reaction times provided the rate constant  $k=7.0\times 10^{-3} \text{ s}^{-1}$  (at 22 °C).

Comparatively, **AuNP-2** is much more active in the catalytic reduction of 4-nitrophenol by sodium borohydride than AuNPs capped with monosubstituted triazole–PEG, which is attributed to the small size of **AuNP-2** and possibly also to the ready displacement of disubstituted triazole ligands by the substrates. All in all, the triazole-stabilized AuNPs reveal a remarkable catalytic activity in the reduction of 4-nitrophenol, which is largely due to the flexibility of the mild AuNP–triazole bonding.

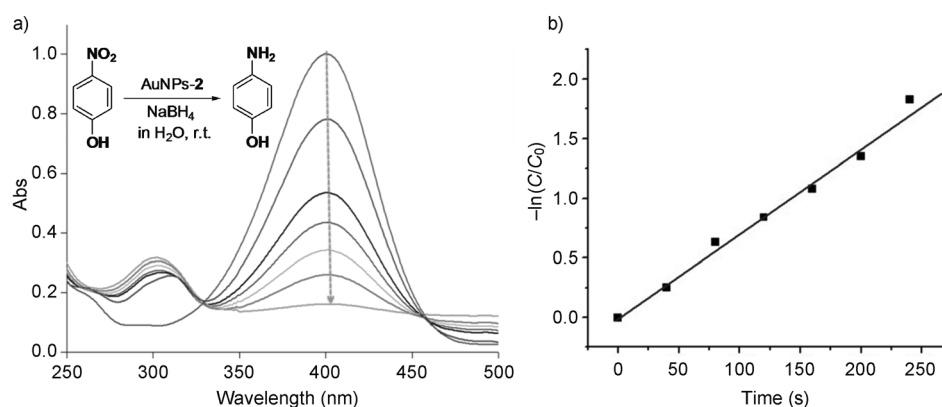


**Figure 5.** a) UV/Vis spectra in which the reaction is monitored every 40 seconds (at 22 °C). b) Consumption rate of 4-nitrophenol  $-\ln(C/C_0)$  versus reaction time.

#### Encapsulation of the hydrophobic compound 1-adamantanol with AuNP-10

The encapsulation properties of **AuNP-10** containing  $\beta$ -CD were investigated by titration of **AuNP-10** into 1-adamantanol (AD) in solution (Figure 6).

First, AD and **AuNPs-10** were separately prepared in  $\text{D}_2\text{O}/[\text{D}_6]\text{DMSO}$  (7:3; 5 mM in each case), followed by the stepwise titration of **AuNP-10** into the solution of AD. After being mixed by inversion, the obtained solution with various molar ratios of AD/ $\beta$ -CD (1:0.5, 1:1, or 1:1.5) was monitored by  $^1\text{H}$  NMR spectroscopic analysis (see the full-scale spectra in Figure S54 in the Supporting Information).

Three characteristic peaks of AD at  $\delta=2.25$ , 1.82, and 1.75 ppm for  $\text{H}_{\gamma}$ ,  $\text{H}_{\beta}$ , and  $\text{H}_{\delta}$ , respectively, showed chemical-shift changes due to the chemical environment of the protons in AD as a result of the formation of the  $\beta$ -CD/AD host–guest inclusion complex formed by trapping AD inside the  $\beta$ -CD cavity (Figure 6). The largest shifts for these three peaks ( $\delta=2.36$ , 1.87, and 1.78 ppm for  $\text{H}_{\gamma}$ ,  $\text{H}_{\beta}$ , and  $\text{H}_{\delta}$ ) were observed in the AD/ $\beta$ -CD ratio of 1:1.5, and no further shift emerged when more **AuNP-10** was added.

This result is in accord with reports of this well-documented host–guest inclusion phenomena.<sup>[20]</sup> Moreover, no SPB shift was observed in the UV/Vis spectrum before and after the association (see Figure S52 in the Supporting Information). This study suggests that **AuNP-10** could potentially be used as a promising drug carrier in cancer therapy without the need to chemically modify a drug because most commercially available drugs are hydrophobic compounds. The delivery potential of such drugs by  $\beta$ -CD and other carriers is well known, and the combination of this species in a AuNP cargo has been highlighted for combined diagnosis and therapy.<sup>[21]</sup>

#### Conclusion

Nanogold chemistry has benefitted from the widespread use of “click” chemistry, which not only stabilizes AuNPs, but also provides a remarkably mild coverage that permits uses and applications that are more difficult to conduct with thiolate-type anionic ligands. The series of disubstituted 1,2,3-triazoles syn-

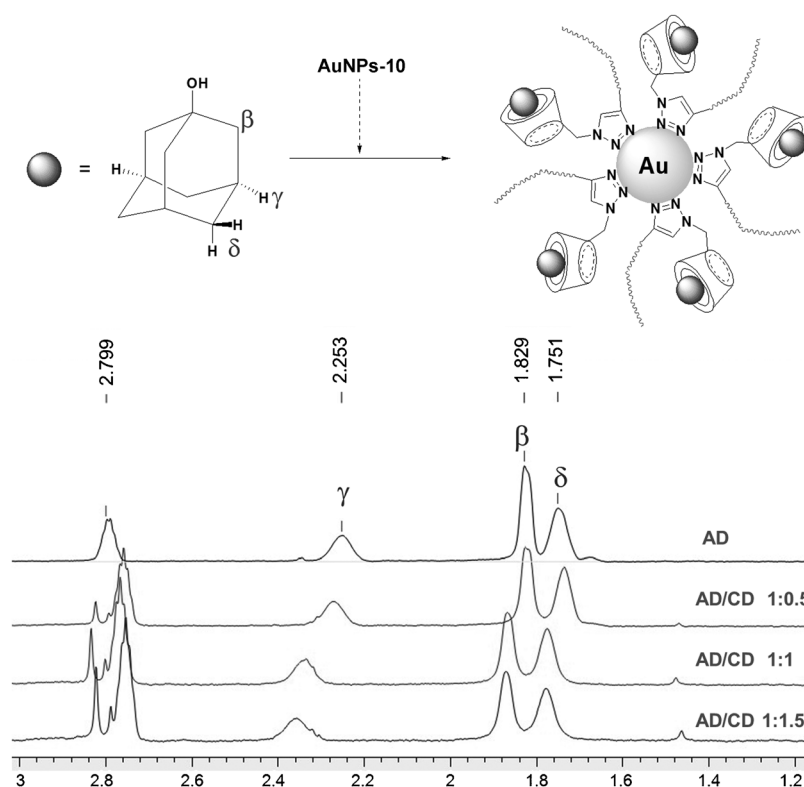


**Figure 6.** Illustration of AD encapsulation with PEG-triazole-cyclodextrin stabilized **AuNP-10**.  $^1\text{H}$  NMR spectra of AD (in  $\text{D}_2\text{O}/[\text{D}_6]\text{DMSO}$  (7:3),  $25^\circ\text{C}$ ) and AD mixed with various amounts of **AuNP-10** after titration (molar ratios of AD/CD = 1:0.5, 1:1, and 1:1.5).

thesized in this study by using straightforward CuAAC “click” reactions contain a PEG chain, which contributes to the water solubility and biocompatibility of the triazole-stabilized AuNPs, and a polymer, dendron, alcohol, carboxylic acid, tris-allyl dendron, fluorescent dye, ferrocene complex, or  $\beta$ -CD moiety. The range of AuNP sizes obtained (i.e., 3.0–11.2 nm) leads to a size-dependent selective choice of applications. The SERS properties of the triazole–AuNPs have been illustrated by comparing the Raman spectrum of **AuNP-5** and **5**, thus providing evidence that the triazole ring was very close to AuNPs surface, that is to say, coordinated. The stability of these triazole–AuNPs under the physiological pH range 4–9 suggests that they are qualified to be used in further studies in the cellular environment, in particular because of the PEG tail, which is not only biocompatible but also provides enhanced permeability and a retention (EPR) effect. The fluorescence-emission decrease of **AuNP-6** relative to ligand **6** alone as a result of the quenching effect of AuNPs successfully designated the **AuNPs-6** as a fluorescent sensor of the sulfur-mustard analogue 2-CEMS. In catalysis, the facile removal of the triazole ligands by the substrate from the small **AuNP-2** (3.0 nm core) is responsible for faster catalysis in the reduction of 4-nitrophenol ( $k = 7.0 \times 10^{-3} \text{ s}^{-1}$ , when 0.5% AuNPs is employed) than with thiolate AuNPs from which thiolate-ligand removal is more difficult. Finally, the excellent encapsulation ability of the trapping of hydrophobic molecules of **AuNP-10** has a potential application in biomedicine.

In summary, this new general strategy that involves the use of common click chemistry to stabilize PEG-tailed bifunctional AuNPs with clicked 1,2,3-triazole ligands opens promising applications toward sensing, supramolecular encapsulation, synthesis of highly functionalized thiolate–AuNPs, and catalysis of various types of reactions.

## Experimental Section

### CuAAC click synthesis of triazoles 1–10

PEG ( $M_w = 2000$ ) azide or PEG-alkyne (1 g, 0.5 mmol) and a given amount of a specific alkyne or azide were dissolved in THF (10 mL).  $\text{CuSO}_4 \cdot 5\text{H}_2\text{O}$  (0.25 mmol, 62 mg) in aqueous solution was added to the reaction mixture, followed by the dropwise addition of a freshly prepared aqueous solution of sodium ascorbate (0.5 mmol, 99 mg) to obtain a THF/water in a ratio of 1:1. The solution was stirred overnight at room temperature under nitrogen. After removal of THF in vacuo,  $\text{CH}_2\text{Cl}_2$  (5 mL) and concentrated (30%) aqueous ammonia solution (5 mL) were added to the reaction mixture, which was stirred for 30 min to remove the Cu ions trapped inside the polymer as  $[\text{Cu}(\text{NH}_3)_2(\text{H}_2\text{O})_2]^{2+}$ . The organic layer was collected and washed with water. After drying with anhydrous  $\text{Na}_2\text{SO}_4$ , the solvent was removed in vacuo. Compounds 1–9 were obtained as white powders in high yields (> 95%) after reprecipitation. Compound **10** was synthesized by using the click reaction between the alkyne (1 g, 0.5 mmol) and azide (580 mg, 0.5 mmol) moieties in water/DMSO (1:1), with CuI (11.6 mg, 0.06 mmol) as the catalyst. The catalyst was subsequently removed by filtration.

### Synthesis of 1,2,3-triazole-mPEG-capped AuNPs 1–10

**General procedure for the synthesis of the AuNPs 1–6, 9, and 10:** Tetrachloroaurate acid (8.5 mg, 0.025 mmol) and the triazole ligand (0.05 mmol; 0.125 and 0.0125 mmol for **AuNPs-2** and **AuNPs-6**, respectively) were dissolved in deionized water (10 mL), and the obtained solution was stirred for 10 min. Freshly prepared sodium borohydride (0.1 mmol) aqueous solution (1 mL) was added dropwise to the reaction mixture with vigorous stirring for 5 min. **AuNPs-7** and **-8** were prepared with a reverse addition to avoid reduction of the  $\text{Au}^{\text{III}}$  center by the ferrocenyl groups. An aqueous solution of tetrachloroaurate acid (5 mL, 8.5 mg, 0.025 mmol) was added dropwise to aqueous solutions of the triazole derivative (6 mL, 0.05 mmol) and sodium borohydride (6 mL, 0.1 mmol). After further stirring for 30 min, the AuNPs were purified by dialysis for 24 h to remove the excess ligands and salts. The triazole–AuNPs were kept in aqueous solution at  $22^\circ\text{C}$ .

### Fluorescence detection of 2-CEMS with AuNPs-6

A gradually increasing amount of 2-chloroethyl methyl sulfide (40 mM; 0.5, 1, 2, 3, 4, 5, 7, 10, 15 and 20 equivalents) in methanol was added to a solution of **AuNPs-6** (2.5 mL, 0.08 mM) in water/methanol (3:7) in a standard quartz cuvette (path length = 1 cm), and monitored directly by fluorescence spectroscopic analysis. The solution with 10 equivalents of analyte (50  $\mu$ L) was monitored after 5, 10, and 20 min, respectively.

### Catalytic reduction of 4-nitrophenol with AuNPs-2

An aqueous solution (2.5 mL) containing 4-nitrophenol (0.09  $\mu$ mol) and NaBH<sub>4</sub> (7.2  $\mu$ mol) was prepared in a standard quartz cuvette (3 mL, path length = 1 cm). The AuNP catalyst (0.5%, 0.45  $\times 10^{-3}$   $\mu$ mol) was injected into this solution, and the reaction progress was detected by UV/Vis spectroscopic analysis every 40 s at 22 °C.

### Encapsulation of 1-adamantanol in AuNPs-10

Solutions of AD and **AuNP-10** were prepared separately in D<sub>2</sub>O/[D<sub>6</sub>]DMSO (7:3, 5 mM in each case), followed by the dropwise titration of the **AuNP-10** solution into the AD solution. After mixing by inversion, solutions of AD and  $\beta$ -CD in various molar ratios (1:0, 1:0.5, 1:1, and 1:1.5) were studied by <sup>1</sup>H NMR spectroscopic analysis.

### Acknowledgements

Financial support from the China Scholarship Council (CSC) (Ph.D. grants to N.L.), the Universities of Bordeaux and Toulouse III, the CNRS, and L'Oréal is gratefully acknowledged.

**Keywords:** click chemistry · fluorescence · gold · nanoparticles · reduction · sulfur-mustard analogues

- [1] a) M. R. Jones, K. D. Osberg, R. J. MacFarlane, M. R. Langille, C. A. Mirkin, *Chem. Rev.* **2011**, *111*, 3736–3827; b) N. J. Halas, S. Lal, W. S. Chang, S. Link, P. Nordlanser, *Chem. Rev.* **2011**, *111*, 3913–3961; c) L. M. Liz-Marzán, *Chem. Commun.* **2013**, *49*, 16–18; d) N. Li, P. Zhao, D. Astruc, *Angew. Chem.* **2014**, *126*, 1784–1818; *Angew. Chem. Int. Ed.* **2014**, *53*, 1756–1789.
- [2] a) M. Haruta, *Nature* **2005**, *437*, 1098–1099; b) A. Corma, P. Serna, *Science* **2006**, *313*, 332–334; c) M. Stratakis, H. Garcia, *Chem. Rev.* **2012**, *112*, 4469–4506; d) Y. Zhang, X. Cui, F. Shi, Y. Deng, *Chem. Rev.* **2012**, *112*, 2467–2505.
- [3] a) C. M. Cogley, J. Chen, E. C. Cho, L. V. Wang, Y. Xia, *Chem. Lett. Chem. Soc., Rev.* **2011**, *40*, 44–56; b) K. Saha, S. S. Agasti, C. Kim, X. Li, V. M. Rotello, *Chem. Rev.* **2012**, *112*, 2739–779; c) H. Jans, Q. Huo, *Chem. Soc. Rev.* **2012**, *41*, 2849–2866.
- [4] a) R. A. Sperling, P. Rivera Gil, M. Zhang, W. J. Parak, *Chem. Lett. Chem. Soc., Rev.* **2008**, *37*, 1896–1908; b) R. Bardhan, S. Lal, A. Joshi, N. J. Halas, *Acc. Chem. Res.* **2011**, *44*, 936–946; c) S. Rana, A. Bajaj, R. Mout, V. M. Rotello, *Adv. Drug Deliv. Rev.* **2012**, *64*, 200–216; d) S. E. Lohse, C. J. Murphy, *J. Am. Chem. Soc.* **2012**, *134*, 15607–15620.
- [5] a) J. Turkevich, P. C. Stevenson, J. Hillier, *Discuss. Faraday Soc.* **1951**, *11*, 55–75; b) G. Frens, *Nature Phys. Sci.* **1973**, *241*, 20–22; c) J. Kimling, M. Maier, B. Okenve, V. Kotaidis, H. Ballot, A. Plech, *J. Phys. Chem. B* **2006**, *110*, 15700–15707; d) S. D. Perrault, W. C. W. Chan, *J. Am. Chem. Soc.* **2009**, *131*, 17042–17043.
- [6] a) M. Brust, M. Walker, D. Bethell, D. J. Schiffrin, R. Whyman, *J. Chem. Soc. Chem. Commun.* **1994**, 801–802; b) M. J. Hostetler, J. E. Wingate, C. J. Zhong, J. E. Harris, R. W. Vachet, M. R. Clark, J. D. Londono, S. J. Green, J. J. Stokes, G. D. Wignall, G. L. Glish, M. D. Porter, N. D. Evans, R. W. Murray, *Langmuir* **1998**, *14*, 17–30; c) B. Hvolbæk, T. V. W. Janssens, B. S. Clausen, H. C. Falsig, H. Christensen, J. K. Nørskov, *Nanotoday* **2007**, *2*, 14–18.
- [7] a) B. Nikoobakht, M. A. El-Sayed, *Chem. Mater.* **2003**, *15*, 1957–1962; b) J. Pérez-Juste, I. Pastoriza-Santos, L. M. Liz-Marzán, P. Mulvaney, *Coor. Chem. Rev.* **2005**, *249*, 1870–1901; c) K. Kwon, K. Y. Lee, Y. W. Lee, M. Kim, J. Heo, S. J. Ahn, S. W. Han, *J. Phys. Chem. C* **2007**, *111*, 1161–1165.
- [8] a) J. L. Ferry, P. Craig, C. Hexel, P. Sisco, R. Frey, P. L. Pennington, M. H. Fulton, I. G. Scott, A. W. Decho, S. Kashiwada, C. J. Murphy, T. Shaw, *J. Nat. Nanotechnol.* **2009**, *4*, 441–444; b) A. M. Alkilany, C. J. Murphy, *J. Nanopart. Res.* **2010**, *12*, 2313–2333; c) N. Khlebtsov, L. Dykman, *Chem. Soc. Rev.* **2011**, *40*, 1647–1671.
- [9] a) C. J. Serpell, J. Cookson, D. Ozkaya, P. D. Beer, *Nat. Chem.* **2011**, *3*, 478–483; b) R. C. Knighton, M. R. Sambrook, J. C. Vincent, S. A. Smith, C. J. Serpell, J. Cookson, M. S. Vichers, P. D. Beer, *Chem. Commun.* **2013**, *49*, 2293–2295; c) C. J. Serpell, J. Cookson, A. L. Thompson, C. M. Brown, P. D. Beer, *Dalton Trans.* **2013**, *42*, 1385–1393.
- [10] a) A. Yu, Z. Liang, J. Cho, F. Caruso, *Nano Lett.* **2003**, *3*, 1203–1207; b) A. Devadoss, A.-M. Spehar-Délèze, D. A. Tanner, P. Bertocello, R. Marthi, T. E. Keyes, R. J. Forster, *Langmuir* **2010**, *26*, 2130–2135; c) H. Lange, J. Maultzsch, W. Meng, D. Mollenhauer, B. Paulus, N. Peica, S. Schlecht, C. Thomsen, *Langmuir* **2011**, *27*, 7258–7264.
- [11] a) C. Kinnear, H. Dietsch, M. J. D. Clift, C. Endes, B. Rothen-Rutishauser, A. Petri-Fink, *Angew. Chem.* **2013**, *125*, 1988–1992; *Angew. Chem. Int. Ed.* **2013**, *52*, 1934–1938; b) S. Rucareanu, V. J. Gandubert, R. B. Lennox, *Chem. Mater.* **2006**, *18*, 4674–4680; c) R. P. Briñas, M. Maetani, J. J. Barchi Jr., *J. Colloid Interf. Sci.* **2013**, *392*, 415–421.
- [12] a) V. V. Rostovtsev, L. G. Green, V. V. Fokin, K. B. Sharpless, *Angew. Chem.* **2002**, *114*, 2708–2711; *Angew. Chem. Int. Ed.* **2002**, *41*, 2596–2599; b) M. Meldal, C. W. Tornøe, *Chem. Rev.* **2008**, *108*, 2952–3015; c) J. E. Hein, V. V. Fokin, *Chem. Soc. Rev.* **2010**, *39*, 1302–1315; d) L. Liang, D. Astruc, *Coord. Chem. Rev.* **2011**, *255*, 2933–2945.
- [13] a) R. A. Sperling, W. J. Parak, *Phil. Trans. R. Soc. A* **2010**, *368*, 1333–1383; b) A. Gole, C. J. Murphy, *Langmuir* **2008**, *24*, 266–272; c) J. L. Brennan, N. S. Hatzakis, T. R. Tshikhudo, N. Dirvianskyte, V. Razumas, S. Patkar, J. Vind, A. Svendsen, R. J. Nolte, A. E. Rowan, M. Brust, *Bioconjugate Chem. Bioconj. Chem.* **2006**, *17*, 1373–1375; d) Y. Zhou, S. Wang, X. Jiang, *Angew. Chem.* **2008**, *120*, 7564–7566; *Angew. Chem. Int. Ed.* **2008**, *47*, 7454–7456.
- [14] a) K. E. Sapsford, W. R. Algar, L. Berti, K. B. Gemmill, E. Oh, M. H. Stewart, I. L. Medintz, *Chem. Rev.* **2013**, *113*, 1904–2074; b) B. Pergolese, M. Muniz-Miranda, A. Bigotto, *J. Phys. Chem. B* **2004**, *108*, 5698–5702; c) A. A. Jbarah, A. Ihle, K. Banert, R. Holze, *J. Raman Spectrosc.* **2006**, *37*, 123–131.
- [15] E. Boisselier, A. K. Diallo, L. Salmon, C. Ornelas, J. Juiz, D. Astruc, *J. Am. Chem. Soc.* **2010**, *132*, 2729–2742.
- [16] a) J.-R. Hamon, D. Astruc, P. Michaud, *J. Am. Chem. Soc.* **1981**, *103*, 758–766; b) A. Heller, *Acc. Chem. Res.* **1990**, *23*, 128–126; c) D. Astruc, *Electron transfer and radical processes in transition metal chemistry*, Wiley-VCH, Weinheim, **1995**, Chapter 7.
- [17] a) M. Daniel, J. Ruiz, S. Nlate, J. C. Blais, D. Astruc, *J. Am. Chem. Soc.* **2003**, *125*, 2617–2628; b) F. Otón, A. Espinosa, A. Tárraga, C. R. de Arelano, P. Molina, *Chem. Eur. J.* **2007**, *13*, 5742–5725.
- [18] L. A. Patil, A. R. Bari, M. D. Shinde, V. Deo, M. P. Kaushik, *Sens. Act. B* **2012**, *161*, 372–380.
- [19] P. Hervés, M. Pérez-Lorenzo, L. M. Liz-Marzán, J. Dzubiella, Y. Lu, M. Balauuff, *Chem. Prod. Chem. Soc., Rev.* **2012**, *41*, 5577–5587.
- [20] a) P. Mukhopadhyay, A. Wu, L. Isaacs, *J. Org. Chem.* **2004**, *69*, 6157–6164; b) H. Goto, Y. Furusho, E. Yashima, *J. Am. Chem. Soc.* **2007**, *129*, 109–112.
- [21] a) C. Burda, X. Chen, M. A. El-Sayed, *Chem. Rev.* **2005**, *105*, 1025–1102; b) C. J. Murphy, A. M. Gole, J. W. Stone, P. N. Sisco, A. M. Alkilany, E. C. Goldsmith, S. C. Baxter, *Acc. Chem. Res.* **2008**, *41*, 1721–1730;

Received: March 18, 2014

Published online on May 30, 2014